# Antimycobacterial Activity of Bioactive Compounds from Eucalyptus globulus against Mycobacterium tuberculosis Aspartate-semialdehyde Dehydrogenase: In silico Analysis

**Jimoh Salamah Mopelola**
salamahjimoh@gmail.com

University of Ilorin
**Memunat Alake Bankole**
Ladoke Akintola University of Technology
**Nurudeen Owolabi**
Ladoke Akintola University of Technology
**Ibrahim Ajadi**
Kwara State University

**Research Article**

**Keywords:** Tuberculosis, Eucalyptus globulus, Antimycobacterial activity, In silico drug discovery, ADMET

**Posted Date:** August 22nd, 2025

**DOI:** https://doi.org/10.21203/rs.3.rs-7337220/v1



**Additional Declarations:** No competing interests reported.

## Abstract

# Background

Tuberculosis is the leading cause of death from a single infectious agent worldwide. Tuberculosis accounted for around 1.25 million deaths globally in 2023. The rise of Multidrug-resistant tuberculosis and the reported side effects of these available anti-TB drugs has complicated the control of the disease. This highlights the urgent need to discover and develop safer and more effective therapies for tuberculosis. *Eucalyptus globulus* is a tree widely distributed across tropical and subtropical regions with numerous medicinal benefits.

# Results

The antimycobacterial potential of *Eucalyptus globulus* against *Mycobacterium tuberculosis* Aspartate-semialdehyde dehydrogenase (ASADH); an enzyme responsible for the bacterium's growth and virulence was accessed using in silico studies. Fifteen bioactive compounds from *Eucalyptus globulus* were selected based on literature. Isoniazid; a first line anti-TB drug was used as our control. SwissADME online server was used to evaluate pharmacokinetic properties of the compounds. The compounds were further prepared to obtain the best docking poses using LigPrep module in the Maestro's Schrodinger software. The compounds were docked into the protein's active site using Schrödinger's Maestro software's Glide module and the resulting protein-ligand complexes was studied. Drug-likeness screening showed that only M-cymene violated Lipinski's rule. Molecular docking revealed that thymol (-5.445) and sabinyl acetate (-5.097) has a higher docking score than isoniazid (-5.040), indicating a better binding affinity and biological activity against the target compared to the control (-5.040). Hydrogen bonds interaction of suggesting high strength of binding and molecular interactions that occurred between the protein-ligand complexes suggesting a strong antimycobacterial inhibitory effect.

# Conclusions

In silico analysis from this study identifies thymol and sabinyl acetate from *Eucalyptus globulus* as promising candidates for further development as anti-TB treatments and show better docking with the target protein compared to isoniazid.

## BACKGROUND

Tuberculosis (TB), caused by *Mycobacterium tuberculosis*, is the deadliest disease resulting from a single infectious agent (1) and one of the oldest diseases known to affect humans (2). Poverty significantly contributes to the persistence of tuberculosis worldwide (3). Nearly a quarter of the world's population has been infected with TB, with a 5–10% lifetime risk of developing TB disease. In 2023, approximately 1.25 million deaths from TB were reported. India, Indonesia, China, the Philippines, Pakistan, Nigeria, Bangladesh, and the Democratic Republic of the Congo accounted for more than two-thirds of global TB cases (4).

Isoniazid and rifampicin (RFP) are first-line medications used to treat tuberculosis (5). Isoniazid, also known as isonicotinic acid hydrazide (INH), is a prodrug that suppresses the growth of mycobacteria (6). Although its precise mechanism of action is not fully understood, it targets fatty acid synthetase in mycobacteria, which plays a role in mycolic acid biosynthesis—essential for cell wall formation (Bereda, 2022). Rifampicin inhibits bacterial DNA-dependent RNA synthesis by targeting bacterial RNA polymerase (6). However, TB treatment becomes significantly more complex due to the emergence of multidrug-resistant (MDR), extensively drug-resistant (XDR), and totally drug-resistant (TDR) strains of *Mycobacterium tuberculosis* (7). Resistance to at least both INH and RIF is classified as multidrug-resistant TB (MDR-TB), while additional resistance to fluoroquinolones and aminoglycosides is referred to as extensively drug-resistant TB (XDR-TB). Global data from 2023 indicates that 400, 000 people developed multidrug- or rifampicin-resistant tuberculosis (MDR/RR-TB) (WHO,2023). The improper use of antimycobacterial medications has contributed to the widespread emergence of multidrug-resistant (MDR) and extensively drug-resistant (XDR) tuberculosis. Patients with MDR-TB are essentially untreatable with standard first-line TB medications.

Resistance to INH arises mainly due to mutations of katG gene which is responsible for encoding catalase-peroxidase, an enzyme responsible for activating isoniazid inside bacterial cell. Among these, the Ser315Thr (S315T) mutation is the most frequently observed, occurring in around 40% of resistant strains. This mutation results in a catalase-peroxidase enzyme that is unable to activate isoniazid, rendering the drug ineffective. However, despite losing its ability to activate the drug, the mutated enzyme retains

approximately half of its normal catalase-peroxidase activity. This residual activity allows the bacterium to maintain oxidative stress defense mechanisms, enabling it to neutralize host-derived antibacterial radicals (8, 9). Rifampicin resistance is most commonly observed in strains that are also resistant to isoniazid, making it a reliable indicator for identifying multidrug-resistant (MDR) *Mycobacterium tuberculosis* strains (9). Rifampicin inhibits RNA synthesis by targeting DNA-dependent RNA polymerase. Resistance to rifampicin is due to mutations of the rpoB gene which encodes the β-subunit of RNA polymerase (10).

As a result, the rise of MDR-TB presents a serious public health challenge, especially in high-burden regions, highlighting the urgent need for the discovery and development of safer and more effective tuberculosis treatments.

Phytochemicals are naturally occurring plant compounds with various therapeutic benefits. They have long been utilized for their medicinal properties and remain a crucial healthcare solution for people in rural areas with limited access to modern medicine and technology (11). Numerous plant-derived drugs have been developed to treat a range of diseases. Advancements in analytical techniques and methodologies have accelerated the discovery of bioactive compounds from plants (12). Given their broad applications, accessibility, and safety as well as the growing prevalence of antibiotic-resistant bacteria (13), there is increasing interest in researching, enhancing, and applying these plant-derived compounds to combat antibiotic-resistant bacterial strains (14, 15).

*Eucalyptus globulus* is a woody shrub or flowering tree belonging to the Myrtaceae family. This aromatic plant is native to Australia and is widely distributed across tropical and subtropical regions (16). Its therapeutic properties are primarily found in its essential oil, which is extracted from the leaves (17). This oil is rich in phytochemicals, including tannins, saponins, terpenoids, glycosides, alkaloids, phenolic compounds, steroids, cardiac glycosides, terpenes, reducing sugars, carbohydrates, resins, acidic compounds, and flavonoids (18). Key constituents of *Eucalyptus globulus* essential oil include 1,8-cineole, α-pinene, γ-terpinene, α-phellandrene, β-pinene, limonene, camphene, and sabinene (19, 20).

Eucalyptus essential oil has a long history of use in traditional medicine for treating respiratory conditions such as colds, coughs, runny nose, sore throat, asthma, nasal congestion, bronchitis, and sinusitis. It is also known for its diverse biological activities, including antibacterial, antioxidant, anticancer, diaphoretic, disinfectant, antimalarial, antiseptic, antidiabetic, analgesic, anti-inflammatory, and expectorant properties (17, 18, 20, 21). Additionally, eucalyptus essential oil and its primary component, 1,8-cineole, have demonstrated strong antibacterial effects, particularly against the biofilm formation of methicillin-resistant *Staphylococcus aureus* (MRSA) strains (21).

Aspartate-semialdehyde dehydrogenase (ASADH) is a crucial enzyme involved in the biosynthesis of amino acids and the cell wall of microorganisms. This enzyme catalyzes the reduction and dephosphorylation of aspartyl-phosphate to aspartate-semialdehyde within the aspartate biosynthetic pathway (22). Aspartate-semialdehyde can subsequently be reduced to homoserine, which serves as a precursor for the synthesis of methionine, threonine, and isoleucine—all of which are essential amino acids. Alternatively, when aspartate-semialdehyde undergoes condensation with pyruvate and cyclization within the aspartate pathway, it forms dihydrodipicolinate, which is further converted into diaminopimelate (23). Diaminopimelate (DAP) is a key metabolite required for the cross-linking of peptidoglycan polymers during bacterial cell wall synthesis (24). Additionally, S-adenosylmethionine, another important product of this pathway, acts as a precursor for quorum-sensing molecules in Gram-negative bacteria, playing a vital role in virulence and infection. Given its essential role in the survival and virulence of *Mycobacterium tuberculosis*, the ASADH enzyme represents a promising drug target for the development of novel antimicrobial therapies.

An increasingly important strategy in drug discovery involves the use of in silico studies (25, 26). This computational approach predicts how molecular ligands interact with protein targets to form stable complexes. In silico methods are widely employed in drug discovery due to their cost-effectiveness, time efficiency, and high predictive accuracy (27). Therefore, this study aimed to evaluate the *Mycobacterium tuberculosis* inhibitory potential of bioactive compounds from *Eucalyptus globulus* by targeting Aspartate-semialdehyde dehydrogenase (ASADH) using an in silico approach.

# METHODS

## Ligand Selection

Bioactive compounds obtained from *Eucalyptus globulus* essential oil was used in this study. Fifteen (15) bioactive compounds including cineole (2758), alpha-phellandrene (CID: 7460), D-Limonene (CID: 440917), m-cymene (CID: 10812), terpinen-4-ol (CID: 11230), globulol (CID: 12304985), spathulenol (CID: 92231), carvacrol (CID: 10364), carvotanacetone (CID: 6432475), thymol (CID:

6989 ), linalool (CID: 6549), 6-Camphenol (CID: 180537), 6-Camphenone (CID: 14088350 ), piperitone (CID: 6987) and Sabinyl acetate (CID: 94266) from eucalyptus essential oil were selected based on literature survey(19, 20). Isoniazid (CID; 3767) was selected as the control ligand. The selected bioactive compounds and control ligands are shown in Table 1. The 3D structures of all the ligands molecules in structure data format (SDF) and canonical SMILES were obtained from the PubChem database (https://pubchem.ncbi.nlm.nih.gov) (28).

Table 1
Selected bioactive compounds and the control drug

| S/N | Name | CID | FORMULA | CANONICAL SMILES |
|---|---|---|---|---|
| 1 | Cineole | 2758 | $C_{10}H_{18}O$ | CC1(C2CCC(O1)(CC2)C)C |
| 2 | Alpha-Phellandrene | 7460 | $C_{10}H_{16}$ | CC1 = CCC(C = C1)C(C)C |
| 3 | D-Limonene | 440917 | $C_{10}H_{16}$ | CC1 = CCC(CC1)C(= C)C |
| 4 | M-cymene | 10812 | $C_{10}H_{14}$ | CC1 = CC(= CC = C1)C(C)C |
| 5 | Terpinen-4-ol | 11230 | $C_{10}H_{18}O$ | CC1 = CCC(CC1)(C(C)C)O |
| 6 | Globulol | 12304985 | $C_{15}H_{24}O$ | CC1CCC2C1C3C(C3(C)C)CCC2(C)O |
| 7 | Spathunelol | 92231 | $C_{15}H_{24}O$ | CC1(C2C1C3C(CCC3(C)O)C(= C)CC2)C |
| 8 | Carvacrol | 10364 | $C_{10}H_{14}O$ | CC1 = C(C = C(C = C1)C(C)C)O |
| 9 | Carvotanacetone | 6432475 | $C_{10}H_{16}O$ | CC1 = CCC(CC1 = O)C(C)C |
| 10 | Thymol | 6989 | $C_{10}H_{14}O$ | CC1 = CC(= C(C = C1)C(C)C)O |
| 11 | Linalool | 6549 | $C_{10}H_{18}O$ | CC(= CCCC(C)(C = C)O)C |
| 12 | 6-Camphenol | 180537 | $C_{10}H_{16}O$ | CC1(C2CC(C1 = C)C(C2)O)C |
| 13 | 6-Camphenone | 14088350 | $C_{10}H_{14}O$ | CC1(C2CC(C1 = C)CC2 = O)C |
| 14 | Piperitone | 6987 | $C_{10}H_{16}O$ | CC(C)C12CC1C(= C)C(C2)OC(= O)C |
| 15 | Sabinyl acetate | 94266 | $C_{12}H_{18}O_2$ | CC(C)C12CC1C(= C)C(C2)OC(= O)C |
| 16 | Isoniazid | 3767 | $C_6H_7N_3O$ | C1 = CN = CC = C1C(= O)NN |

## Protein Target Selection

The target protein, *Mycobacterium tuberculosis* Aspartate-semialdehyde dehydrogenase (ASADH) was selected using literature (29). The 3D crystal structures of the protein (PDB: 3TZ6) in the form of atomic coordinates was obtained from Protein Data Bank (https://www.rcsb.org) (30). Figure 1 shows the structure of *Mycobacterium tuberculosis* Aspartate-semialdehyde dehydrogenase (ASADH).

## Protein targets preparation

The 3D crystallized structure of the target protein; *Mycobacterium tuberculosis* Aspartate-semialdehyde dehydrogenase (ASADH), was accomplished using the protein preparation module of Schrödinger's molecular modeling suit. Protein preparation was carried out by removal of unwanted water molecules, heteroatoms, and co-crystallized ligands coordinates to obtain a more suitable and stable conformation. The protein was minimized for molecular docking using OPLS 4 force field and saved in PDB format.

## Active Site Generation

The grid orientation of the active site was simulated from the binding conformation of the target protein co-crystallized ligand using the grid module of Schrödinger's molecular modeling suit. X, Y, Z coordinates of the gird box are 238.99, 50.38, and 75.95 respectively.

## Drug-likeness Screening

The fifteen (15) bioactive compounds and the two control drugs were screened for their drug likeness properties using the SwissADME (http://swissadme.ch/ ) online server. These compounds were subjected to drug-likeness screening using the parameters hypothesized by Lipinski, Verber, and Egan. Fourteen (14) out of the fifteen (15) selected bioactive compounds did not violate Lipinski rule and were subjected to molecular docking.

# Ligand Preparation

The fourteen screened compounds were imported into the LigPrep workflow. OPLS4 forcefield was used due its accuracy in obtaining improved docking poses and conformational analyses (31). Tautomers were generated for each ligand and the PH specified for generation of ionization state was 7.0 +_ 2.0

## Molecular Docking

Grid module of Schrödinger's molecular modeling suit was used to for molecular docking of the protein target and ligands. The prepared ligands and the generated grid file were imported into the program. Standard Precision (SP) docking mode was used and docking was performed flexibly.

## ADMET Evaluation

The absorption, distribution, metabolism, excretion and toxicity (ADMET) of the top ligands obtained from the molecular docking and the control was evaluated using ADMETLab online server (https://admetmesh.scbdd.com/service/evaluation/cal) (32). The pharmacokinetic properties were then predicted from the results.

## RESULTS

# Drug-likeness Screening

Drug likeness screening results as shown in Table 2 indicated that only M-cymene out of the fifteen bioactive compounds selected from Eucalyptus essential oil violated Lipinski's drug likeness rule and was therefore eliminated for further analysis. The control ligand; Isoniazid passed the drug likeness screening. The remaining fourteen compounds that passed the drug-likeness screening and the control ligand were subjected for docking analysis with *Mtb*-ASADH.

# Molecular Docking

Results from the molecular docking study of the fourteen bioactive compounds that passed the drug-likeness screening and the control ligand revealed their docking score, ligand interaction, as well as their hydrogen binding affinities.

The results of the bioactive compounds from eucalyptus plant presented in Table 3 predicts their binding affinity and suggest potential biological activity against the target protein *Mtb*-ASADH. Docking score indicates that thymol (-5.445) had the highest docking score, followed by Sabinyl acetate (-5.097). These two ligands had a higher docking score than Isoniazid (-5.040) indicating a better binding affinity and potential biological activity against the target. Amino acids residues observed in the hydrogen bond interaction of sabinyl acetate with the target protein were Asn 94 and Arg 99 while amino acids residues observed with the hydrogen bond interaction of thymol with the target protein were Arg 99, Asn 94 and Lys 227.

Figure 2 shows the interaction of thymol, sabinyl acetate and isoniazid with the target.

Table 2
Screening results of drug-likeness bioactive compounds and control drug using SwissADME web tool

| Molecule | MW | XLOGP | TPSA | Lipinski #Violation | Ghose #Violation | Veber #Violation | Egan Violation | Meugge #Violation | Bioavalability Score |
|---|---|---|---|---|---|---|---|---|---|
| Cineole | 154.25 | 2.74 | 9.23 | 0 | 1 | 0 | 0 | 2 | 0.55 |
| Alpha-Phellandrene | 136.23 | 3.21 | 0 | 0 | 1 | 0 | 0 | 2 | 0.55 |
| D-Limonene | 136.23 | 4.57 | 0 | 0 | 1 | 0 | 0 | 2 | 0.55 |
| M-cymene | 134.22 | 4.5 | 0 | 1 | 1 | 0 | 0 | 2 | 0.55 |
| Terpinen-4-ol | 154.25 | 3.26 | 20.23 | 0 | 1 | 0 | 0 | 2 | 0.55 |
| Globulol | 222.37 | 3.74 | 20.23 | 0 | 0 | 0 | 0 | 1 | 0.55 |
| Spathunelol | 220.35 | 3.11 | 20.23 | 0 | 0 | 0 | 0 | 1 | 0.55 |
| Carvacrol | 150.22 | 3.49 | 20.23 | 0 | 1 | 0 | 0 | 2 | 0.55 |
| Carvotanacetone | 152.23 | 2.5 | 17.07 | 0 | 1 | 0 | 0 | 2 | 0.55 |
| Thymol | 150.22 | 3.3 | 20.23 | 0 | 1 | 0 | 0 | 2 | 0.55 |
| Linalool | 154.25 | 2.97 | 20.23 | 0 | 1 | 0 | 0 | 2 | 0.55 |
| 6-Camphenol | 152.23 | 1.78 | 20.23 | 0 | 1 | 0 | 0 | 2 | 0.55 |
| 6-Camphenone | 150.22 | 1.5 | 17.07 | 0 | 1 | 0 | 0 | 2 | 0.55 |
| Piperitone | 152.23 | 2.85 | 17.07 | 0 | 1 | 0 | 0 | 2 | 0.55 |
| Sabinyl acetate | 194.27 | 2.36 | 26.3 | 0 | 0 | 0 | 0 | 1 | 0.55 |
| Isoniazid | 137.14 | 0.7 | 68.01 | 0 | 3 | 0 | 0 | 1 | 0.55 |

Table 3
Molecular docking score of the bioactive compounds and the control drug

| S/N | Name | CID | Docking Score |
|---|---|---|---|
| 1 | Cineole | 2758 | -4.294 |
| 2 | Alpha-Phellandrene | 7460 | 4.986 |
| 3 | D-Limonene | 440917 | -3.849 |
| 4 | M-cymene | 10812 | -4.715 |
| 5 | Terpinen-4-ol | 11230 | -4.799 |
| 6 | Globulol | 12304985 | -4.470 |
| 7 | Spathunelol | 92231 | -4.519 |
| 8 | Carvacrol | 10364 | -4.901 |
| 9 | Carvotanacetone | 6432475 | -4.956 |
| 10 | Thymol | 6989 | -5.445 |
| 11 | Linalool | 6549 | |
| 12 | 6-Camphenol | 180537 | -4.552 |
| 13 | 6-Camphenone | 14088350 | -4.689 |
| 14 | Piperitone | 6987 | -4.982 |
| 15 | Sabinyl acetate | 94266 | -5.097 |
| 16 | Isoniazid | 3767 | -5.040 |

# ADMET STUDY

The predicted absorption, distribution, metabolism, excretion, and toxicity (ADMET) profiles of the two top-scoring bioactive compounds, in comparison with the control drug, are presented in Table 4. For classification model endpoints such as blood-brain barrier permeability (BBB), human intestinal absorption (H-HT), and hERG channel inhibition, prediction probabilities were categorized into six symbolic levels: 0–0.1 (−−−), 0.1–0.3 (−−), 0.3–0.5 (−), 0.5–0.7 (+), 0.7–0.9 (++), and 0.9–1.0 (+++). Generally, '+++' or '++' indicates a higher likelihood of toxicity or undesired effects, whereas '−−−' or '−−' suggests that the molecule is likely to be nontoxic or favorable (Xiong et al., 2021).

Regarding absorption and distribution, all top-hit compounds, including the control, were predicted to cross the blood-brain barrier (BBB). The predicted plasma protein binding (PPB) values were expressed as percentages. Sabinyl acetate and thymol exhibited PPB values of 47.56% and 93.90%, respectively, whereas isoniazid had a PPB value of 9%.

In terms of metabolism, sabinyl acetate posed a lower risk of cytochrome P450 (CYP)-related drug interactions, as it showed no inhibition for any of the tested CYP enzymes. Thymol exhibited no inhibition for three out of the five tested CYP enzymes. Isoniazid, on the other hand, showed inhibition specifically for the CYP1A2 enzyme.

The predicted elimination half-life ($t_1/_2$) values provided insights into drug excretion rates. Thymol has a half-life of 0.098, sabinyl acetate; 0.0682 while isoniazid had a half-life of 0.715.

In terms of toxicity, none of the compounds demonstrated hERG inhibition, indicating a lower risk of cardiac side effects. Additionally, all compounds tested negative in the Ames mutagenicity assay, suggesting a lack of mutagenic potential. Furthermore, none of the top-hit compounds exhibited rat oral acute toxicity. However, sabinyl acetate was predicted to have carcinogenic potential.

Table 4
ADMET profiling of Drug Candidates and Control Drugs

| ADMET MODELS | Isoniazid | Thymol | Sabinyl acetate |
|---|---|---|---|
| **Absorption & Distribution** | | | |
| HIA | --- | --- | --- |
| P-gp substrate | --- | --- | --- |
| PPB | 9.00% | 93.90% | 47.56% |
| **Metabolism** | | | |
| CYP1A2 inhibitor | ++ | +++ | -- |
| CYP2C19 inhibitor | -- | ++ | --- |
| CYP2C9 inhibitor | --- | - | --- |
| CYP2D6 inhibitor | -- | ++ | --- |
| CYP3A4 inhibitor | - | -- | -- |
| **Excretion** | | | |
| T1/2 | 0.715 | 0.682 | 0.098 |
| **Toxicity** | | | |
| Ames toxicity | --- | --- | --- |
| Carcinogenicity | -- | -- | ++ |
| Rat oral acute toxicity | ++ | -- | - |
| H-HT | - | --- | -- |
| DILI | +++ | -- | ++ |
| hERG blockers | --- | --- | --- |
| Respiratory toxicity | + | + | +++ |
| SR-p53 | --- | --- | + |

# DISCUSSION

## Drug-likeness screening

The drug-likeness rules are important in discriminating ideal drug-like compounds from false positives. This assertion is supported by a study conducted by (33). The drug likeness properties of the bioactive compounds and the control were determined using Lipinski's, Ghose's, Veber's, Egan's and Muegge's drug likeness rule. The top rank hit bioactive compounds for this study was selected from compounds that passed at least three out of the five rules. These drug-likeness rules are major determinants of oral bioavailability potential of any drug molecule i.e., the probability of drug molecule being readily available to target tissues after being absorbed into the body system. This concept is correlated with previous studies(34–36). The control in this study; isoniazid, violated two of the rules. Sabinyl acetate, thymol and the rest of the bioactive compounds excluding M-cymene passed at least three of the drug-likeness rules including the Lipinski's rule of five indicating that these compounds can potentially be suitable for oral use. Lipinski's rule is a set of conditions that defines oral bioavailability of a compound based on its chemical and physical properties of the compound (37–39). According to the rule, a drug is considered to be suitable for oral activity if it has no more than five hydrogen bond donors, no more than ten hydrogen bond acceptors, molecular mass ≤ 500 Daltons and an octanol water partition co-efficient (XlogP) not greater than five. Saganuwan (40), reported that the molecular mass of a compound exerts an influence on a compound's efficacy as a drug, the molecular weight of a drug determines its oral use and cellular permeability. Bioactive compound with molecular weight within the Lipinski's range has an optimal permeability that makes it easy to cross cellular membranes and reach its target within a short time. XlogP is a measure of a compound's hydrophobicity and it represents the ratio of the concentration of a compound in octanol to its

concentration in water. XlogP is a relevant parameter that influences the drug-likeness property of a compound by determining its permeability through cell membranes and thereby aiding their absorption(41). The result presented in Table 1 indicates that the top hit selected bioactive compounds in this study has a good druggability and can be used as oral drugs.

# Molecular docking

Molecular docking result indicated that all 14 compounds selected for the study docked to the active site of the target protein. However, Sabinyl acetate and thymol were the only ligands with docking score higher than the control. The docking score of Sabinyl acetate and thymol was − 5.097 and − 5.445 and respectively while the docking score of the Isoniazid was − 5.040 as shown in Table 1. This observation indicates a strong binding affinity between *Mycobacterium Tuberculosis* ASADH and the two bioactive compounds and suggests that these compounds can effectively interact with ASADH, inhibit its action, modulate its function and elicit a potentially strong therapeutic action. Previous studies have reported that binding affinity reflects the strength of interaction and the ability of ligand molecules to modulate biological functions (42, 43). Furthermore, Sabinyl acetate interacted with *Mycobacterium Tuberculosis* ASADH active site with 2 hydrogen bonds at amino acid residues; Arg99 and Asn94, Thymol interacted with the protein's active site with 1 hydrogen bond at amino acid residue; Arg99, while isoniazid interacted with the protein's active site with 3 hydrogen bonds at amino acid residue; Arg99, Lys227 and Asn94. The H-bond interactions observed in Sabinyl acetate and thymol indicates a high degree of binding and molecular interactions between the protein-ligand complex. This suggests a high degree of binding activity and molecular interaction. This aligns with previous studies (44–46) that reported hydrogen bond is fundamental, enhances stability and essential of effective binding. Moreover, the amino acid residues in the key active site of the protein interacting with the ligands through hydrogen bonding correlates with the studies done by (47, 48) where they showed that Arg99, Lys227 and others are the interacting amino acid residues of *Mtb*-ASADH. Therefore, binding the compounds to *Mtb*-ASADH could offer some antimycobacterial effects in tuberculosis treatment by the inhibition of *Mtb*-ASADH. Figures 1 and 2 shows interaction of compound in sabinyl acetate, thymol and isoniazid with *the target protein*.

# ADMET

The absorption, distribution, metabolism, excretion and toxicity profiles of abinyl acetate, thymol and the control are presented in Table 3. ADMET profiling is very essential because it determines the pharmacokinetics of our hit compounds, analyzes its possible action in the body and helps assess its efficacy (49).

Human intestinal absorption (HIA) is a crucial parameter in evaluating the oral bioavailability of a compound, as it determines how effectively a drug enters the systemic circulation following administration. High HIA is generally associated with improved absorption, enhanced therapeutic efficacy, and a more favorable dosing regimen (50). In this study, both thymol and sabinyl acetate were predicted to have favorable levels of HIA, indicating absorption through the gastrointestinal tract. This may increase their suitability for oral delivery as antimycobacterial agents.

Another important pharmacokinetic property is blood–brain barrier (BBB) permeability, which restricts the entry of compounds into the central nervous system (CNS) (51) and presents a major challenge in treating infections such as CNS tuberculosis (CNS-TB), a severe and often fatal manifestation of TB caused by the infiltration of Mycobacterium species into the CNS (52). Both thymol and sabinyl acetate, along with the control drug isoniazid, were predicted to be BBB permeant, suggesting that they have the ability to cross the BBB and may therefore be effective in the treatment of CNS-TB.

Plasma protein binding (PPB) is another important factor influencing the pharmacokinetics of drug candidates, as it determines the fraction of drug available in its free, active form to interact with the biological target. Proteins such as serum albumin and α1-acid glycoprotein are known to bind a wide range of drugs, often affecting their efficacy. In general, a PPB value exceeding 90% can reduce the amount of free drug available and potentially attenuate its therapeutic effect. In this study, sabinyl acetate exhibited a moderate PPB score of 47.56%, indicating that a significant proportion of the compound remains unbound and available for therapeutic action. Isoniazid showed a low PPB score of 9.00%, further confirming its availability in free form. Thymol, however, had a high PPB score of 93.90%, which may limit its immediate bioavailability. Nonetheless, studies suggest that high PPB does not always correlate directly with reduced potency, as several clinically effective drugs exhibit high plasma protein binding yet retain strong pharmacological activity(53).

The cytochrome P450 (CYP) family of enzymes, primarily expressed in the liver, plays a central role in drug metabolism. Inhibition of these enzymes can lead to drug–drug interactions, reduced drug clearance, accumulation of toxic metabolites, or decreased therapeutic efficacy (54). In this study, sabinyl acetate was predicted not to inhibit any of the major CYP isoforms, suggesting a low

potential for enzyme-related interactions. Thymol was also predicted not to inhibit CYP3A4, one of the most clinically significant isoforms. These findings indicate that both compounds are unlikely to cause CYP-mediated drug–drug interactions, thereby supporting their metabolic stability and safety in potential combination therapies.

Half-life is another critical pharmacokinetic parameter that reflects the duration a drug remains active in the body and influences dosing frequency. Based on empirical classification, compounds with a half-life between 0 and 0.3 hours are considered to have excellent metabolic clearance, those between 0.3 and 0.7 hours are moderate, while values between 0.7 and 1.0 hours are considered poor (41).Thymol and sabinyl acetate recorded half-lives of 0.098 and 0.0682 respectively, which fall within the excellent category, suggesting rapid clearance from the system. This indicates favorable metabolic processing.

In terms of toxicity, both thymol and sabinyl acetate demonstrated favorable safety profiles. The two compounds showed low predicted binding affinity to the human ether-à-go-go-related gene (hERG) potassium channel, which plays a vital role in the repolarization of cardiac cells. Inhibition of this channel can result in delayed cardiac repolarization, leading to conditions such as long QT syndrome (LQTS), arrhythmias, and Torsade de Pointes (TdP) (55). The low hERG inhibition scores suggest a reduced risk of cardiotoxicity, making both compounds safer for potential therapeutic use. Furthermore, all three compounds, including the control, were Ames-negative, indicating a low likelihood of causing DNA mutations, and therefore a reduced risk of carcinogenicity or heritable genetic damage. In addition, thymol and sabinyl acetate were predicted to be non-hepatotoxic, signifying minimal potential for liver damage or dysfunction, which further supports their safety for therapeutic development. However, it is important to note that sabinyl acetate was predicted to be carcinogenic, unlike thymol and isoniazid, which were both classified as non-carcinogenic. Thus, the findings of this study suggest that the active compounds thymol and sabinyl acetate may exhibit strong in silico inhibitory activity against *Mycobacterium tuberculosis* aspartate-semialdehyde dehydrogenase, as evidenced by molecular docking analysis. However, these computational results require further validation through molecular dynamics simulations and experimental (in vitro and in vivo) studies to confirm their therapeutic potential.

## CONCLUSIONS

Tuberculosis (TB) remains the leading cause of death from a single infectious agent globally. The emergence of multidrug-resistant TB (MDR-TB) has intensified the urgency to develop more effective and safer therapeutic alternatives. This study evaluated the antimycobacterial potential of bioactive compounds derived from *Eucalyptus globulus* against *Mycobacterium tuberculosis* aspartate-semialdehyde dehydrogenase, using isoniazid, a frontline anti-TB drug, as the control. Drug-likeness screening and molecular docking analyses identified thymol and sabinyl acetate as the top-performing compounds, both demonstrating strong binding affinity and stable hydrogen interactions with the *Mtb*-ASADH. ADMET profiling further supported their potential as promising drug candidates. The compounds were predicted to cross the blood–brain barrier, showed no significant inhibition of cytochrome P450 enzymes, and exhibited favorable half-lives. Although thymol displayed high plasma protein binding and sabinyl acetate showed carcinogenic potential, their overall pharmacokinetic and safety profiles suggest a strong therapeutic promise. The findings from this in silico study provide a foundation for further validation through in vitro and in vivo experiments to confirm their efficacy and safety as novel antimycobacterial agents.

## Declarations

**Ethics approval and consent to participate** – Not Applicable

**Consent for publication** – Not Applicable

**Availability of data and materials** – All data generated and analysed during this study are included in this published article.

**Competing interests** – The author(s) declare(s) that they have no competing interests.

**Funding** – Not Applicable

**Authors' contributions** – SMJ designed and executed experiments, performed the docking analysis and wrote the manuscript. MAB and NA designed and executed experiments, obtained protein and ligand structures and edited the manuscript. IA input on data analysis and revised the manuscript. All authors read and approved the final manuscript.

**Acknowledgments** – Not Applicable

## References


1. World Health Organization. Tuberculosis (TB) [Internet]. 2024 [cited 2025 Jun 19]. Available from: https://www.who.int/news-room/fact-sheets/detail/tuberculosis
2. Natarajan A, Beena PM, Devnikar AV, Mali S. A systemic review on tuberculosis. Indian J Tuberc. 2020;67(3):295–311.
3. Hargreaves JR, Boccia D, Evans CA, Adato M, Petticrew M, Porter JDH. The Social Determinants of Tuberculosis: From Evidence to Action. Am J Public Health. 2011;101(4):654–62.
4. World Health Organization. 1.1 TB incidence [Internet]. 2023 [cited 2025 Jun 19]. Available from: https://www.who.int/teams/global-programme-on-tuberculosis-and-lung-health/tb-reports/global-tuberculosis-report-2023/tb-disease-burden/1-1-tb-incidence
5. Bereda G. First Line Anti-Tuberculosis Medication: Current and Ongoing Clinical Management. 2022.
6. Kumar M, Singh SK, Singh PP, Singh VK, Rai AC, Srivastava AK, et al. Potential Anti-Mycobacterium tuberculosis Activity of Plant Secondary Metabolites: Insight with Molecular Docking Interactions. Antioxidants. 2021;10(12):1990.
7. Nahid P, Mase SR, Migliori GB, Sotgiu G, Bothamley GH, Brozek JL, et al. Treatment of Drug-Resistant Tuberculosis. An Official ATS/CDC/ERS/IDSA Clinical Practice Guideline. Am J Respir Crit Care Med. 2019;200(10):e93–142.
8. Ramaswamy S, Musser JM. Molecular genetic basis of antimicrobial agent resistance in*Mycobacterium tuberculosis*: 1998 update. Tuber Lung Dis. 1998;79(1):3–29.
9. Somoskovi A, Parsons LM, Salfinger M. The molecular basis of resistance to isoniazid, rifampin, and pyrazinamide in Mycobacterium tuberculosis. Respir Res. 2001;2(3):164.
10. Telenti A, Imboden P, Marchesi F, Matter L, Schopfer K, Bodmer T, et al. Detection of rifampicin-resistance mutations in Mycobacterium tuberculosis. Lancet. 1993;341(8846):647–51.
11. Garcia-Campoy A, Garcia E, Muñiz-Ramirez A. Phytochemical and Pharmacological Study of the Eysenhardtia Genus. Plants. 2020;9(9):1124.
12. Chihomvu P, Ganesan A, Gibbons S, Woollard K, Hayes MA. Phytochemicals in Drug Discovery—A Confluence of Tradition and Innovation. Int J Mol Sci. 2024;25(16):8792.
13. Abdallah EM, Alhatlani BY, De Paula Menezes R, Martins CHG. Back to Nature: Medicinal Plants as Promising Sources for Antibacterial Drugs in the Post-Antibiotic Era. Plants. 2023;12(17):3077.
14. Thangaraj PMR. Anti-Bacterial Attributes of Phytochemicals from Bougainvillaea spectabilis: Computational Approach. Pharmacogn Res. 2024;16(2):384–90.
15. Tiwana G, Cock IE, Cheesman MJ. Combinations of Terminalia bellirica (Gaertn.) Roxb. and Terminalia chebula Retz. Extracts with Selected Antibiotics Against Antibiotic-Resistant Bacteria: Bioactivity and Phytochemistry. Antibiotics. 2024;13(10):994.
16. Potts B, Vaillancourt R, Jordan GJ, Dutkowski GW, da Costa e Silva J, McKinnon GE et al. Exploration of the Eucalyptus globulus gene pool. 2004 Jan 1 [cited 2025 Jun 19]; Available from: https://figshare.utas.edu.au/articles/conference_contribution/Exploration_of_the_Eucalyptus_globulus_gene_pool/23213207/1
17. Silva J, Abebe W, Sousa SM, Duarte VG, Machado MIL, Matos FJA. Analgesic and anti-inflammatory effects of essential oils of Eucalyptus. J Ethnopharmacol. 2003;89(2):277–83.
18. Mishra AK, Sahu N, Mishra A, Ghosh AK, Jha S, Chattopadhyay P. Phytochemical Screening and Antioxidant Activity of essential oil of Eucalyptus leaf. Pharmacogn J. 2010;2(16):25–8.
19. Shala AY, Gururani MA. Phytochemical Properties and Diverse Beneficial Roles of Eucalyptus globulus Labill. Rev Horticulturae. 2021;7(11):450.
20. Usman LA, Oguntoye OS, Ismaeel RO, Usman LA, Oguntoye OS, Ismaeel RO, PHYTOCHEMICAL PROFILE, ANTIOXIDANT AND ANTIDIABETIC POTENTIAL OF ESSENTIAL OIL FROM FRESH AND DRIED LEAVES OF Eucalyptus globulus. J Chil Chem Soc. 2022;67(1):5453–61.
21. Sharma AD, Farmaha M, Kaur I, Singh N. Phytochemical analysis using GC-FID, FPLC fingerprinting, antioxidant, antimicrobial, anti-inflammatory activities analysis of traditionally used Eucalyptus globulus essential oil. Drug Anal Res. 2021;5(1):26–38.
22. Viola RE. The Central Enzymes of the Aspartate Family of Amino Acid Biosynthesis. Acc Chem Res. 2001;34(5):339–49.
23. Hadfield A, Shammas C, Kryger G, Ringe D, Petsko GA, Ouyang J, et al. Active Site Analysis of the Potential Antimicrobial Target Aspartate Semialdehyde Dehydrogenase. Biochemistry. 2001;40(48):14475–83.

24. van Heijenoort J. Recent advances in the formation of the bacterial peptidoglycan monomer unit. Nat Prod Rep. 2001;18(5):503–19.
25. Roney M, Mohd Aluwi MFF. The importance of in-silico studies in drug discovery. Intell Pharm. 2024;2(4):578–9.
26. Sabe VT, Ntombela T, Jhamba LA, Maguire GEM, Govender T, Naicker T, et al. Current trends in computer aided drug design and a highlight of drugs discovered via computational techniques: A review. Eur J Med Chem. 2021;224:113705.
27. Meng XY, Zhang HX, Mezei M, Cui M. Molecular Docking: A Powerful Approach for Structure-Based Drug Discovery. Curr Comput Aided Drug Des. 2011;7(2):146–57.
28. Kim S, Chen J, Cheng T, Gindulyte A, He J, He S, et al. PubChem in 2021: new data content and improved web interfaces. Nucleic Acids Res. 2021;49(D1):D1388–95.
29. Meng J, Yang Y, Xiao C, Guan Y, Hao X, Deng Q, et al. Identification and Validation of Aspartic Acid Semialdehyde Dehydrogenase as a New Anti-Mycobacterium Tuberculosis Target. Int J Mol Sci. 2015;16(10):23572–86.
30. Berman HM. The Protein Data Bank. Nucleic Acids Res. 2000;28(1):235–42.
31. D'Amore L, Hahn DF, Dotson DL, Horton JT, Anwar J, Craig I, et al. Collaborative Assessment of Molecular Geometries and Energies from the Open Force Field. J Chem Inf Model. 2022;62(23):6094–104.
32. Dong J, Wang NN, Yao ZJ, Zhang L, Cheng Y, Ouyang D, et al. ADMETlab: a platform for systematic ADMET evaluation based on a comprehensively collected ADMET database. J Cheminformatics. 2018;10(1):29.
33. Mahgoub RE, Mohamed FE, Alzyoud L, Ali BR, Ferreira J, Rabeh WM, et al. The Discovery of Small Allosteric and Active Site Inhibitors of the SARS-CoV-2 Main Protease via Structure-Based Virtual Screening and Biological Evaluation. Molecules. 2022;27(19):6710.
34. Mahgoub RE, Mohamed FE, Ali BR, Ferreira J, Rabeh WM, Atatreh N, et al. Discovery of pyrimidoindol and benzylpyrrolyl inhibitors targeting SARS-CoV-2 main protease (Mpro) through pharmacophore modelling, covalent docking, and biological evaluation. J Mol Graph Model. 2024;127:108672.
35. Srivastava V, Yadav A, Sarkar P. Molecular docking and ADMET study of bioactive compounds of Glycyrrhiza glabra against main protease of SARS-CoV2. Mater Today Proc. 2022;49:2999–3007.
36. Halder SK, Elma F. In silico identification of novel chemical compounds with anti-TB potential for the inhibition of InhA and EthR from Mycobacterium tuberculosis [Internet]. Bioinformatics; 2020 [cited 2025 Jun 17]. Available from: http://biorxiv.org/lookup/doi/10.1101/2020.12.04.411967
37. Lipinski CA. Drug-like properties and the causes of poor solubility and poor permeability. J Pharmacol Toxicol Methods. 2000;44(1):235–49.
38. Lipinski CA. Rule of five in 2015 and beyond: Target and ligand structural limitations, ligand chemistry structure and drug discovery project decisions. Adv Drug Deliv Rev. 2016;101:34–41.
39. Lipinski CA, Lombardo F, Dominy BW, Feeney PJ. Experimental and computational approaches to estimate solubility and permeability in drug discovery and development settings. Adv Drug Deliv Rev. 2012;64:4–17.
40. Saganuwan S. Structure-activity relationship of pharmacophores and toxicophores: the need for clinical strategy. Daru J Fac Pharm Tehran Univ Med Sci [Internet]. 2024 [cited 2025 Jun 17]; Available from: https://consensus.app/papers/structureactivity-relationship-of-pharmacophores-and-saganuwan/497397cd29f3587f82fcccf6219706ec/.
41. Xiong G, Wu Z, Fu L, Yang Z, Hsieh C, Yin M, et al. ADMETlab 2.0: an integrated online platform for accurate and comprehensive predictions of ADMET properties. Nucleic Acids Res. 2021;49(W1):W5–14.
42. Friedman R. Computational studies of protein–drug binding affinity changes upon mutations in the drug target. WIREs Comput Mol Sci. 2022;12(1):e1563.
43. Fuji H, Qi F, Qu L, Takaesu Y, Hoshino T. Prediction of Ligand Binding Affinity to Target Proteins by Molecular Mechanics Theoretical Calculation. Chem Pharm Bull (Tokyo). 2017;65(5):461–8.
44. Dhakal A, McKay C, Tanner JJ, Cheng J. Artificial intelligence in the prediction of protein–ligand interactions: recent advances and future directions. Brief Bioinform. 2022;23(1):bbab476.
45. Madushanka A, Moura RT, Verma N, Kraka E. Quantum Mechanical Assessment of Protein–Ligand Hydrogen Bond Strength Patterns: Insights from Semiempirical Tight-Binding and Local Vibrational Mode Theory. Int J Mol Sci. 2023;24(7):6311.
46. Patil R, Das S, Stanley A, Yadav L, Sudhakar A, Varma AK. Optimized Hydrophobic Interactions and Hydrogen Bonding at the Target-Ligand Interface Leads the Pathways of Drug-Designing. Hannenhalli S, editor. PLoS ONE. 2010;5(8):e12029.

47. Kumar R, Garg P, Bharatam PV. Shape-based virtual screening, docking, and molecular dynamics simulations to identify *Mtb* -ASADH inhibitors. J Biomol Struct Dyn. 2015;33(5):1082–93.
48. Kumar R, Garg P, Bharatam PV. Pharmacoinformatics analysis to identify inhibitors of *Mtb* -ASADH. J Biomol Struct Dyn. 2016;34(1):1–14.
49. Daoud NEH, Borah P, Deb PK, Venugopala KN, Hourani W, Alzweiri M, et al. ADMET Profiling in Drug Discovery and Development: Perspectives of In Silico, In Vitro and Integrated Approaches. Curr Drug Metab. 2021;22(7):503–22.
50. Fagerholm U. Prediction of human pharmacokinetics —gastrointestinal absorption. J Pharm Pharmacol. 2007;59(7):905–16.
51. Alavijeh MS, Chishty M, Qaiser MZ, Palmer AM. Drug metabolism and pharmacokinetics, the blood-brain barrier, and central nervous system drug discovery. NeuroRX. 2005;2(4):554–71.
52. Be N, Kim K, Bishai W, Jain S. Pathogenesis of Central Nervous System Tuberculosis. Curr Mol Med. 2009;9(2):94–9.
53. Trainor GL. The importance of plasma protein binding in drug discovery. Expert Opin Drug Discov. 2007;2(1):51–64.
54. Esteves F, Rueff J, Kranendonk M. The Central Role of Cytochrome P450 in Xenobiotic Metabolism—A Brief Review on a Fascinating Enzyme Family. J Xenobiotics. 2021;11(3):94–114.
55. Finlayson K, Witchel HJ, McCulloch J, Sharkey J. Acquired QT interval prolongation and HERG: implications for drug discovery and development. Eur J Pharmacol. 2004;500(1–3):129–42.

## Figures

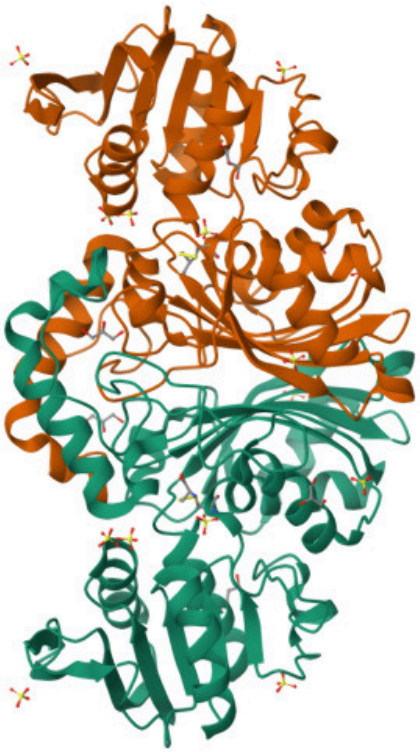

**Figure 1**

Structure of the protein *Mycobacterium tuberculosis* Aspartate-semialdehyde dehydrogenase

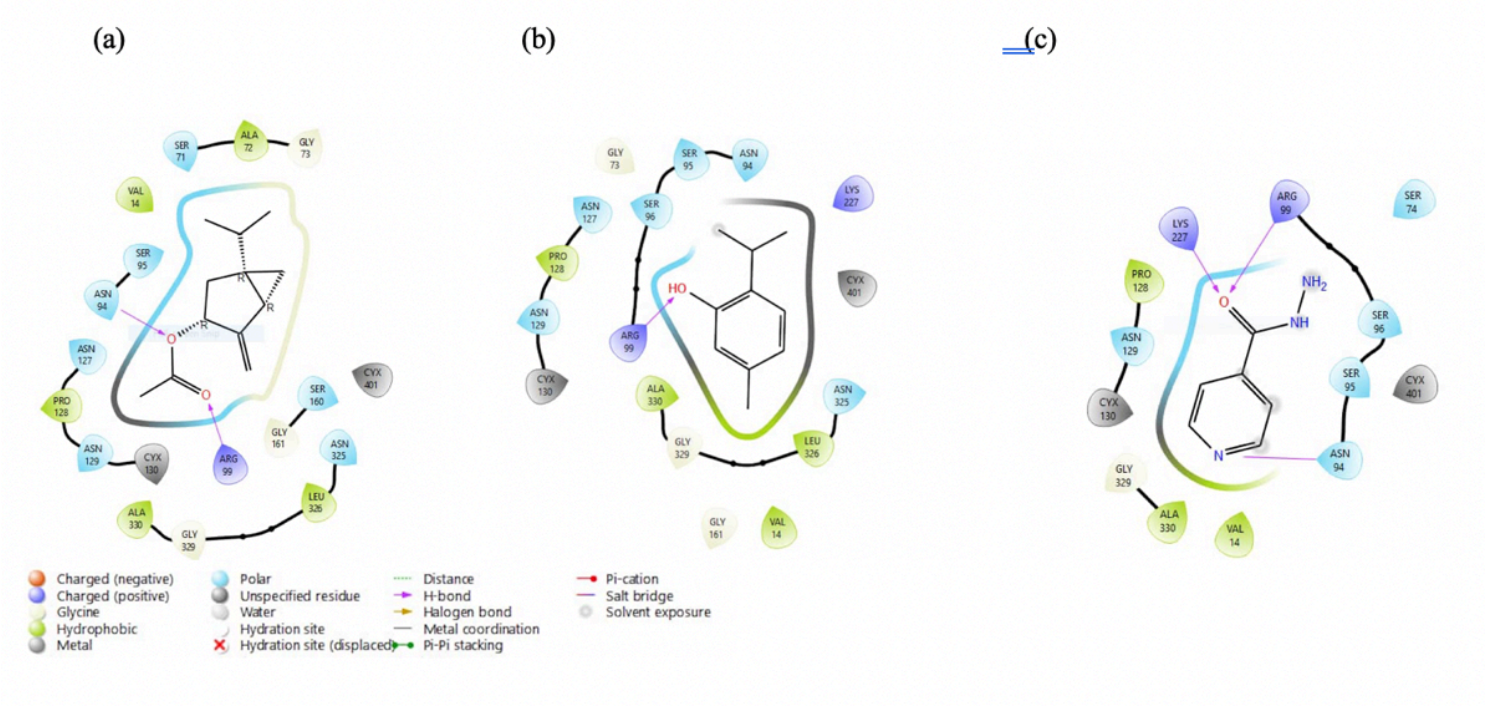


## Figure 2

Binding Configuration of Sabinyl acetate (2a), Thymol (2b) and Isoniazid (2c) in the active site of *Mtb*-ASADH as obtained from molecular docking using Grid module of Schrödinger's molecular modelling suit.